Highly Sensitive and Selective Dynamic Light-Scattering Assay for TNT Detection Using *p*-ATP Attached Gold Nanoparticle

Samuel S. R. Dasary, Dulal Senapati, Anant Kumar Singh, Yerramilli Anjaneyulu, Hongtao Yu, and Paresh Chandra Ray*

Department of Chemistry, Jackson State University, Jackson, Mississippi 39217, United States

ABSTRACT TNT is one of the most commonly used nitro aromatic explosives for landmines of military and terrorist activities. As a result, there is an urgent need for rapid and reliable methods for the detection of trace amount of TNT for screenings in airport, analysis of forensic samples, and environmental analysis. Driven by the need to detect trace amounts of TNT from environmental samples, this article demonstrates a label-free, highly selective, and ultrasensitive para-aminothiophenol (*p*-ATP) modified gold nanoparticle based dynamic light scattering (DLS) probe for TNT recognition in 100 pico molar (pM) level from ethanol:acetonitile mixture solution. Because of the formation of strong π-donor−acceptor interaction between TNT and *p*-ATP, para-aminothiophenol attached gold nanoparticles undergo aggregation in the presence of TNT, which changes the DLS intensity tremendously. A detailed mechanism for significant DLS intensity change has been discussed. Our experimental results show that TNT can be detected quickly and accurately without any dye tagging in 100 pM level with excellent discrimination against other nitro compounds.

KEYWORDS: TNT detection • dynamic light scattering • gold nanoparticle • aggregation • plasmonics • selectivity

INTRODUCTION

Detection of illegally transported explosive materials like 2,4,6-trinitrotoluene has become important for assuring safety at airports and air travel (1−6). TNT is also a major source of hazardous water pollution, which is produced through military preparation of landmines (1−6). As a result, there is an urgent need for rapid and reliable methods of trace detection of TNT, for screenings in airports, analysis of forensic samples, and environmental analysis. These explosive materials must be detected with rapid response time and preferably without any sample preparation. Although current technologies are quite sensitive, often their selectivity is insufficient for performance in practical applications because of false positive signals (1−6). For growing market needs of the 21st century, future devices must link with selectivity, speed, simplicity, and cost-effective (6−30). As a result, different sensor concepts for analyzing TNT have been reported in the last 10 years (7−18), which include nanotechnology-based sensors (7−9, 11−13), electrochemistry-based sensors (10), fluorescence quenching sensors (15), organic dye-based fluorescence resonance energy transfer (FRET) (14), and conjugated polymer-based single and mutiphoton sensors (16−18). But FRET assays identify TNT analyte through a covalently linked label such as a fluorescent or luminescence tag. Necessity of tagging makes it difficult to use them as biosensors for real life. Driven by the need, in this article, we demonstrate that para amino-thiophenol (*p*-ATP)-modified gold-nanoparticle-based dynamic light-scattering (DLS) probe can be used for label-free detection of TNT, with excellent detection limit (100 pm) and selectivity over DNT and other nitrocompounds.

DLS, known as photon correlation spectroscopy (PCS), is a noninvasive, well-established technique for measuring the size of particles ranging in size from 0.5 nm to 6 μm (31−35). DLS is an absolute measurement and it is a powerful tool for determining small change in the size of particles (31−35). Noble metal nanostructures attract great interest because of their unique size- or shape-dependent properties, including large optical field enhancements resulting in the strong scattering and absorption of light (6−30, 36−43). Because of the presence of this surface plasmon resonances, weak scattering effects generally gets significantly enhanced via strong electromagnetic (plasmon) fields at the surfaces of metallic nanostructures (6−30, 36−43). This, together with our ability to make nanomaterials of different sizes and shapes, makes them potentially useful assay for possible daily life applications (6−30, 36−43). Recently, we and other groups have shown that this technique coupled with noble metal nanoparticles can be used in ultrasensitive assay for chemical and bilogical detection, where nanoparticles are used as a light-scattering enhancer and DLS as a read-out system (31−35). In this manuscript, for the first time, we are demonstrating that *p*-ATP-conjugated gold-nanoparticle-based DLS assay can be used for selective detection of TNT.

MATERIALS AND EXPERIMENTS

Hydrogen tetrachloroaurate ($HAuCl_4 \cdot 3H_2O$), sodium citrate, *p*-ATP, 2,6-dinitrotoluene, nitrophenol, acetontrile, and ethanol were purchased from Sigma-Aldrich and used without further purification. 2,4,6-Trinitrotoluene was provided by ERDC, Vicksburg, MS.

* Corresponding author. E-mail: paresh.c.ray@jsums.edu. Fax: 601-979-3674.
Received for review June 12, 2010 and accepted November 1, 2010

DOI: 10.1021/am1005139

Scheme 1. Schematic Representation of *p*-ATP-Conjugated Gold-Nanoparticle-Based TNT Detection: (A) Shematic Representation Showing *p*-ATP Modification Process; (B) Schematic Representation Showing *p*-ATP-Modified Gold Nanoparticle Aggregation in the Presence of TNT

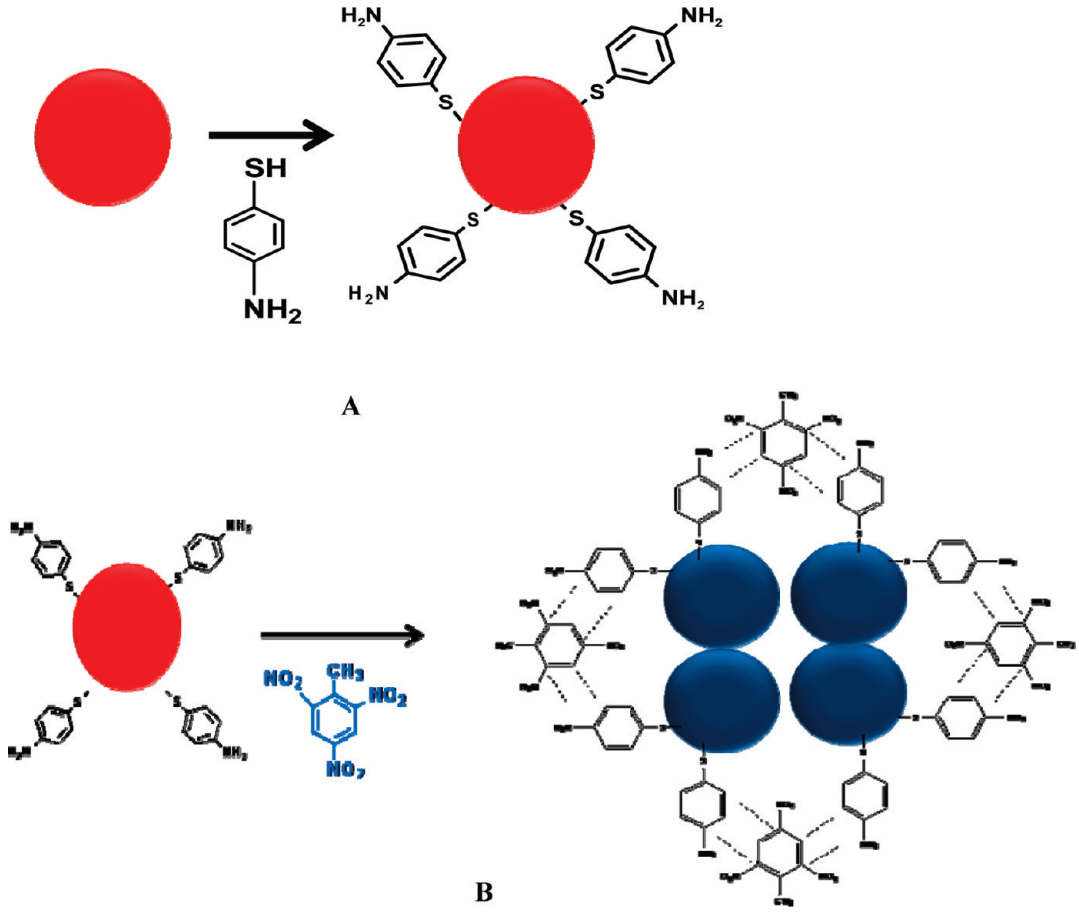

Gold Nanoparticle Synthesis. Gold nanoparticles of 13 nm size was synthesized by using $HAuCl_4$, $3H_2O$ and sodium citrate concentration as we reported recently (9, 21−24, 32). JEM-2100F transmission electron microscope (TEM) and UV−visible absorption spectrum were used to characterize the nanoparticles. The particle concentration was measured by UV−visible spectroscopy using the molar extinction coefficients at the wavelength of the maximum absorption of each gold colloid as reported recently (9, 21−24, 32).

Gold Nanoparticle Surface Modification. For selective detection of TNT, we have modified the gold nanoparticle surface by *p*-ATP 9:1 volume ratio of freshly prepared AuNPs (10 nM) and amino-thiophenol (1×10^{-6} M) was mixed by stirring for 12 h. Excess amino thiophenol was removed by centrifugation at 8000 rpm for several minutes. By using UV−vis absorption spectra, we estimated an average of 15−20 amino thiophenol per gold nanoparticle.

Colorimetric Detection of TNT. Colorimetric detection of TNT was carried out using 675 μL of 9:1 v/v ratio of 1 μM p-ATP anchored GNPs solution (10nM). Then different volumes of TNT stock prepared in 4:1 EtOH/ACN was added to the solution to attain TNT concentrations in the range of 10 nM to 250 μM. The final volume of the solution was adjusted to 750 μL. Samples with other nitro explosives were prepared by substituting TNT. Although the color change was instant, photographs were taken after 30 min of TNT addition for full color development. Photographs were taken using a Cannon S70 digital camera.

Dynamic Light-Scattering Measurement. DLS measurement was performed using Malvern Zetasizer Nano instrument. Conventional DLS becomes ineffective in absorbing media, since the laser beam is absorbed by the sample and can induce an interfering effect. Also, in case of concentrated samples, the artifact of multiple scattering can hamper the measurement. To reduce all the above problems, we used noninvasive backscatter (NIBS) technology (32). DLS detection of TNT was carried out in the range of 100 fM to 250 nM using similar procedures as described above for colorimetric detection. All diameters reported here are based on DLS intensity average using a non-negative least-squares analysis method. For each sample, five DLS measurements were conducted with a fixed 10 runs.

RESULTS AND DISCUSSION

Our detection is based on the fact that in the presence of TNT, *p*-ATP-conjugated gold nanoparticles undergo aggregation (as shown in Scheme 1) because of the π-donor−acceptor interactions between TNT and *p*-ATP-linked gold nanoparticle (11−13), which enabled the binding of TNT and GNP. One TNT molecule can be involved in π-donor−acceptor interactions with several *p*-ATP-attached GNPs (shown in Scheme 1B). As a result, *p*-ATP-attached GNP undergoes aggregation in the presence of TNT and the size of aggregates should increase as we add higher amount of TNT. In our study, we have used *p*-ATP as the primary amine for π-donor−acceptor interaction as well as stabilizer for the gold nanoparticles. After the addition of freshly prepared citrate-stabilized gold nanoparticles, the nanosurfaces were modified by *p*-ATP through the Au−S covalent bond (as

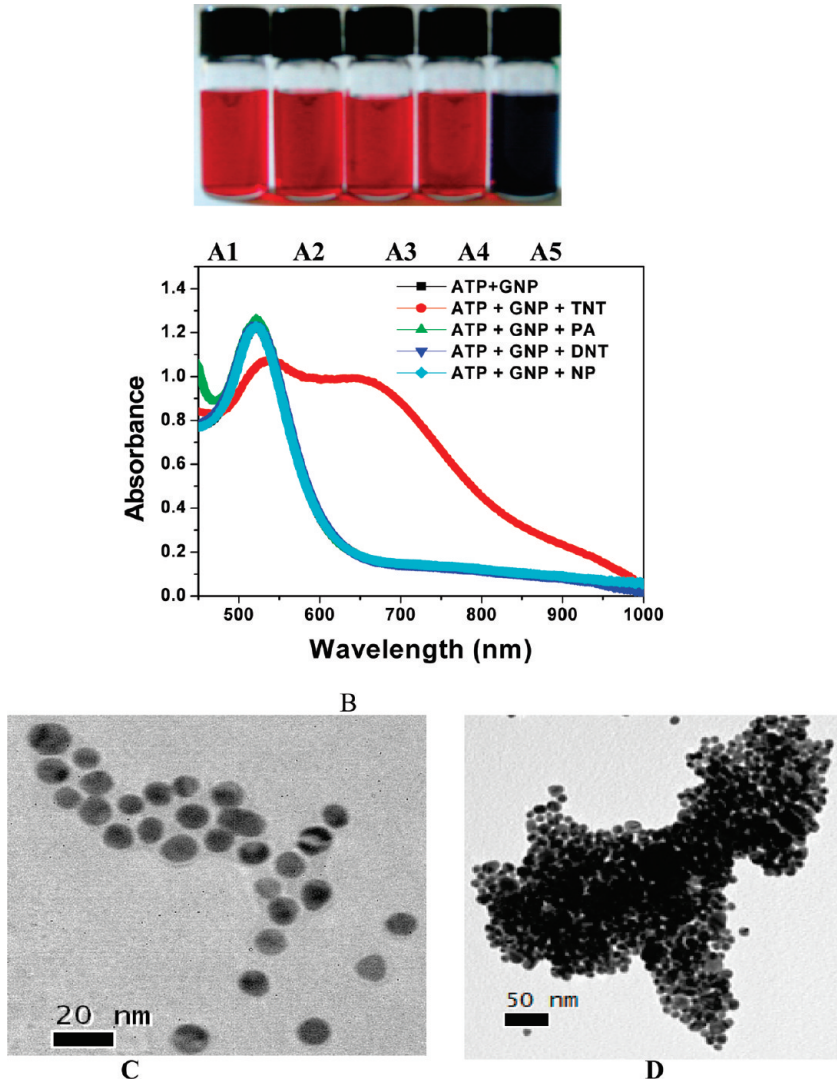

FIGURE 1. (A) Photograph showing colorimetric image of *p*-ATP-conjugated gold nanoparticle (A1) without anything, and in the presence of (A2) 0.3 mM 2,4 dinitro toluene (DNT), (A3) 0.3 mM nitro-phenol (NP), (A4) 0.3 mM picric acid (PA), (A5) 150 μM TNT. (B) Absorption spectral changes of *p*-ATP-modified gold nanoparticle in the presence of TNT. Absorption spectra remain the same in the presence of DNT, NP, or PA. (C) TEM image of p-ATP modified gold nanoparticle in the absence of TNT and D) TEM image of *p*-ATP-modified gold nanoparticle in the presence of TNT.

shown in Scheme 1). The addition of *p*-ATP does not change the color and the absorption spectrum of gold nanoparticle remains the same, which indicates that there is no aggregation when 9:1 volume ratio of freshly prepared AuNPs (10 nM) and *p*-ATP (1×10^{-6} M) was stirred. TEM image of *p*-ATP modified gold nanoparticle, as shown in Figure 1C, also confirmed it.

When we added TNT to *p*-ATP-modified gold nanoparticle, it undergoes aggregation (as shown in Figure 1D) due to the strong π-donor−acceptor interaction between TNT and *p*-ATP, as we discussed before. Aggregation in the presence of TNT ions yields both a substantial shift in the plasmon band energy to longer wavelength and a red-to-blue color change (as shown in Figure 1A,B). This red shift might be due to two factors. One is the change in the local refractive index on the nanoparticle surface caused by the specific binding of the *p*-ATP-conjugated, oval-shaped gold nanoparticles with TNT. The other is the interparticle interaction resulting from the assembly of nanoparticles on surface.

To understand whether our assay is highly selective, we have also performed colorimetric response upon the addition of 2,4 -dinitrotoluene (DNT), 2,4,6-trinitrophenol (TNP), or picric acid (PA) and nitrophenol. Figure 1A shows the colorimetric response of our probe in the presence of various nitro compounds. Figure 1B demonstrates the absorption spectral response in the presence of various organic nitro compounds. Our absorption spectral measurement (as shown in Figure 1B) clearly shows that there are no visible bands between 600 and 800 nm in the presence of 500 μM DNT, PA or NP, whereas we observed very strong absorption bands with peaks at 650 nm in the presence of 200 μM TNT, which is due to the formation of *p*-ATP-conjugated nanoaggregates via strong π-donor−acceptor interaction. This may

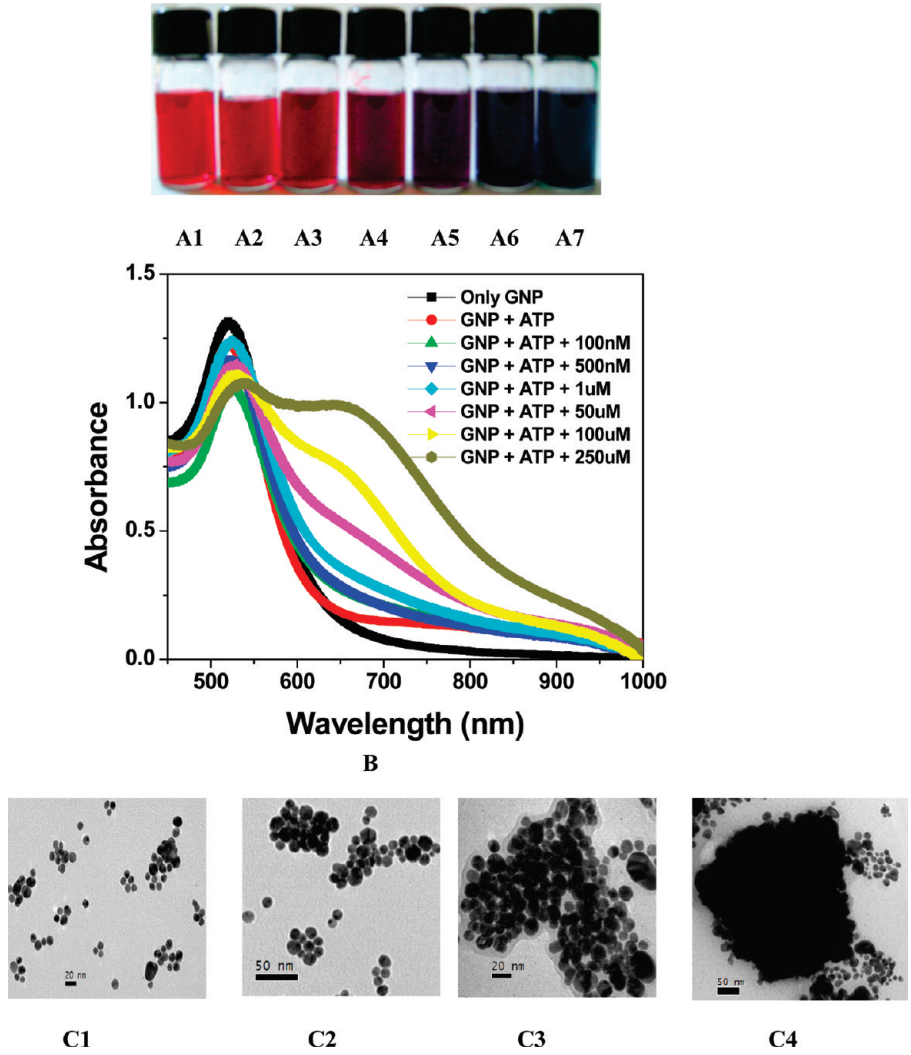

FIGURE 2. (A) Photograph showing colorimetric change upon the addition of different concentrations of TNT on ATP-modified gold nanoparticle: (A1) 1 nM TNT, (A2) 100 nM TNT, (A3) 500 nM TNT, (A4) 1 μM TNT, (A5) 50 μM TNT, (A6) 100 μM TNT, (A7) presence of 250 μM TNT. Our data clearly demonstrate that the sensitivity of colorimetric assay is around 50 μM. (B) The plot demonstrates the absorption spectral changes of ATP-modified gold nanoparticle in the presence of different concentrations of TNT. (C) TEM images showing how gold nanoparticle aggregate sizes vary with the concentration of TNT: (C1) 5 nM TNT, (C2) 100 nM TNT, (C3) 50 μM TNT, (C4) 500 μM TNT.

be due to the fact that the reduction potential for TNT is much lower (−565 mV) than DNT (−674 mV) or TNP (−764 mV) (44).

Our experimental absorption and colorimetric studies clearly demonstrate that *p*-ATP-modified gold nanoparticle does not undergo aggregation in the presence of DNT and other nitro compounds, which allows us to selectively detect TNT. In the case of DNT, because of the lack of a $-NO_2$ group in the fourth position of the benzene ring, partial negative charge may not be distributed throughout the DNT molecular ring. Because of the lack of enough anionic charge, DNT may not form strong π-donor−acceptor interaction like TNT and as a result, the aggregation of *p*-ATP-modified gold nanoparticles is prevented. The same phenomenon is true for nitro phenol. So our result clearly shows excellent selectivity of our probe over DNT, PA, and nitro phenol.

To evaluate the sensitivity of our *p*-ATP-attached gold -nanoparticle-based colorimetric assay, we evaluated different concentrations of TNT from one stock solution. As shown in Figure 2A, our colorimetric assay is highly sensitive to the concentration of TNT. Figure 2B shows how the absorption spectra change with the concentration of TNT. Our experimental results (as shown in Figure 2A) clearly demonstrate that the sensitivity of our colorimetric assay is as low as 50 μM TNT. We have also performed TEM experiment to understand how the cluster size changes with the concentration of TNT. As shown in Figure 2C, our TEM data clearly show that as TNT concentration increases from 5 nm to 500 μM, the nanoaggregate size increases tremendously. Our experimental results also demonstrate that colorimetric response is only visible when the aggregate sizes are quite big.

To improve the assay sensitivity toward TNT detection, we have employed a *p*-ATP-attached gold-nanoparticle-based DLS technique. DLS is a powerful method to determine the small change in the size of the particles. As shown in Figures 3B−D and 2C, when different concentrations of TNT was added to *p*-ATP-modified gold nanoparticles, at a lower concentration of TNT, only a smaller aggregate is formed and as a result, colorimetric assay is not able to

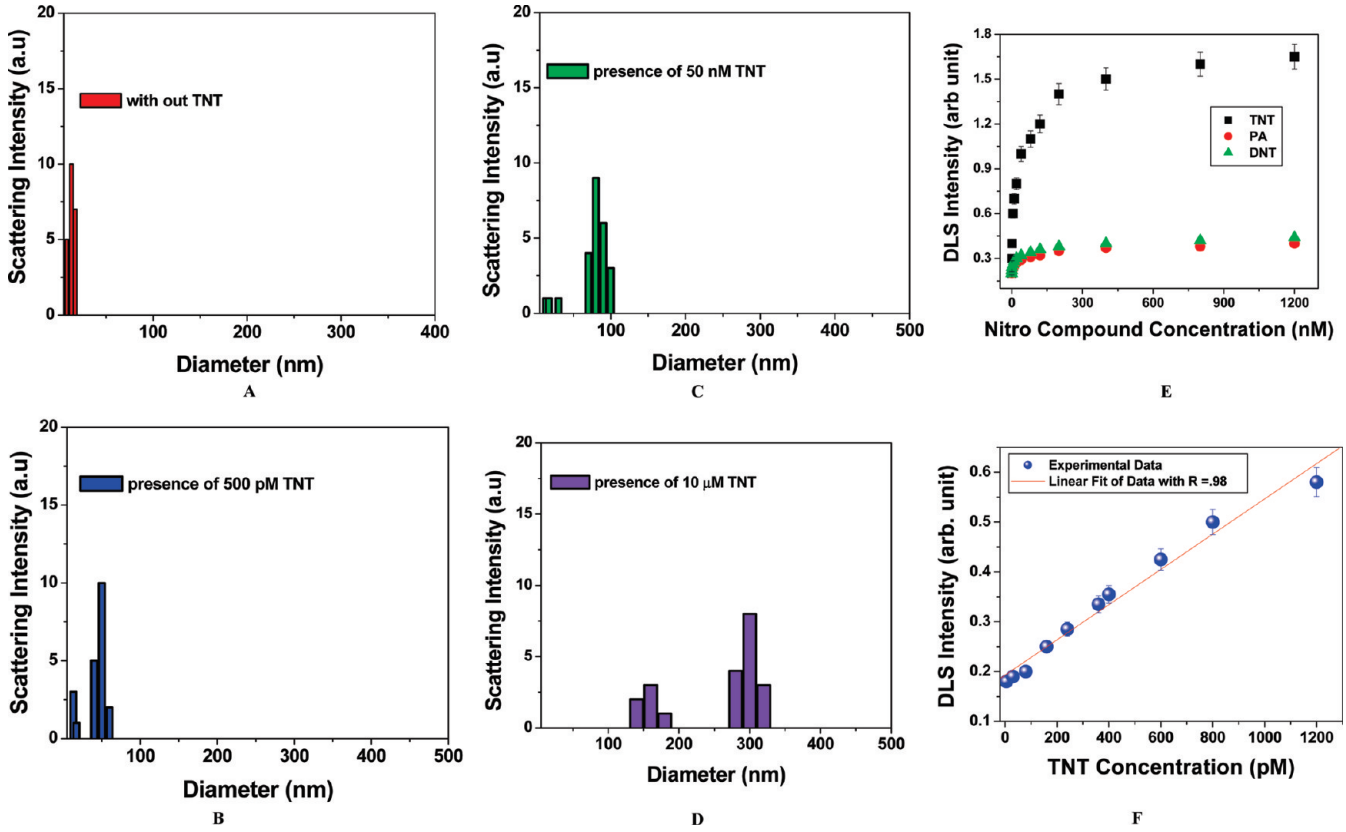

FIGURE 3. Size distributions of *p*-ATP-attached gold nanoparticles measured by DLS: (A) in the absence of TNT, (B) in the presence of 500 pM TNT, (c) in the presence of 15 nM TNT, (D) in the presence of 300 nM TNT. (E) Plot demonstrating how DLS intensity varies with TNT/PA/DNT concentration from 1 pM to 1200 nM. (F) Plot demonstrating how DLS intensity varies with TNT concentration from 1 pM to 1200 pM.

respond. Because DLS has the capability to separate dimers from the monomers (31−35), *p*-ATP-conjugated gold-nanoparticle-based DLS assay should be able to show the response at very low concentration of TNT, when only dimers, trimers, and slightly bigger aggregates are formed. Figure 3 clearly shows that DLS technique is highly sensitive to the concentration of TNT. Our experimental results clearly demonstrate (as shown in Figure 3E,F) that the sensitivity of our DLS assay for TNT detection is as low as 100 pM. Our result shows that DLS assay is about 5 orders of magnitude more sensitive than the usual colorimetric technique. Our experimental results also show that as we increase the concentration of TNT above 300 nM, the DLS intensity remains almost unchanged. It may be due to the fact that as we increase the concentration of TNT, aggregate or cluster size increases. And after certain concentration of TNT, when the size becomes >1 μm, it is close to the saturation point of DLS instrument and as a result, DLS signal remains unchanged.

To understand whether our DLS assay is highly selective, we have also performed DLS experiment with DNT, PA, and NP. Figure 3A shows the *p*-ATP-attached gold-nanoparticle-based DLS response in the presence of different concentrations of various nitro compounds. Our results clearly show that our DLS assay is highly selective for TNT and it can easily separate it from other nitro compounds. We have also tested how stable is our *p*-ATP-attached gold nanoparticle in the presence of trace acid or base contaminants, which change the pH of the solution. We found that *p*-ATP-attached gold nanoparticle is highly stable between pH 5.5 to 8.5, which indicates that presence of trace acid or base contaminants will not perturb our assay activity when pH of the solution in the range of 5.5 to 8.5.

CONCLUSION

In conclusion, in this article, we have demonstrated for the first time a *p*-ATP-conjugated, gold-nanoparticle-based, highly selective, and ultrasensitive DLS probe for the TNT recognition in 100 pM level in aqueous solution. We have shown that because of the formation of strong π-donor−acceptor interaction between TNT and *p*-ATP P, para-amino-thiophenol-attached gold nanoparticles undergo aggregation in the presence of TNT, resulting in a tremendous DLS intensity change. Our experimental results show that TNT can be detected quickly and accurately without any dye tagging in 100 pM level with excellent discrimination against other nitro aromatic compounds. Our experiment also demonstrated that the sensitivity of our DLS assay to detect TNT level in water is about 5 orders of magnitude higher than the colorimetric technique. Our experimental results reported here open up a new possibility for rapid, easy, and reliable diagnosis of TNT from environmental sample by measuring the DLS intensity. Given the simplicity, speed, and sensitivity of this approach, the described methodology could easily be extended to a high-throughput format and become a new method of choice in all applications that require an assay for explosive detection. It is probably possible to improve the our DLS assay sensitivity by several

orders of magnitudes by choosing proper materials and as a result, we still need a much greater understanding on how to control surface architecture in order to stabilize and maximize the DLS response.

Acknowledgment. P.C.R. thanks the Department of Defense (Grant W 912HZ-06-C-0057) and NSF-PREM (Grant DMR-0611539) for their generous funding. We also thank the reviewers, whose valuable suggestions improved the quality of the manuscript.

REFERENCES AND NOTES

(1) Lubin, A. A.; Plaxco, K. W. *Acc. Chem. Res.* **2010**, *43*, 496–505.
(2) Smith, K. D.; McCord, B. R.; MacCrehan, W. A.; Mount, K.; Rowe, W. F. *J. Forensic. Sci.* **1999**, *44*, 789–794.
(3) Thomas III, S. W.; Joly, G. D.; Swager, T. M. *Chem. Rev.* **2007**, *107*, 1339–1386.
(4) Dillewijn, P. V.; Couselo, J. L.; Corredoira, E.; Delgado, A.; Wittich, R. M.; Ballester, A.; Ramos, J. L. *Environ. Sci. Technol.* **2008**, *42*, 7405–7410.
(5) Brettell, T. A.; Butler, J. M.; Almirall, J. R. *Anal. Chem.* **2007**, *79*, 4365–4384.
(6) McQuade, D. T.; Pullen, A. E.; Swager, T. M. *Chem. Rev.* **2000**, *100*, 2537–2574.
(7) Riskin, M.; Tel-Vered, R.; Lioubashevski, O.; Willner, I. *J. Am. Chem. Soc.* **2009**, *131*, 7368–7378.
(8) Aguilar, D. A.; Forzani, E. S.; Leright, M.; Tsow, F.; Cagan, A.; Iglesias, R. A.; Nagahara, L. A.; Amlani, J.; Tsui, R.; Tao, N. J. *Nano Lett.* **2010**, *10*, 380–384.
(9) Dasary, S. S. R.; Singh, A. K.; Senapati, D.; Yu, H.; Ray, P. C. *J. Am. Chem. Soc.* **2009**, *131*, 13806–13812.
(10) Alizadeh, T.; Zare, M.; Ganzali, M. R.; Norouzi, P.; Tavana, B. *Biosens. Bioelectron.* **2010**, *25*, 1166–1172.
(11) Riskin, M.; Tel-Vered, R.; Lioubashevski, O.; Willner, I. *J. Am. Chem. Soc.* **2009**, *131*, 7368–7378.
(12) Riskin, M.; Tel-Vered, R.; Bourenko, T.; Granot, E.; Willner, I. *J. Am. Chem. Soc.* **2008**, *130*, 9726–9733.
(13) Forzani, E. R.; Lu, D.; Leright, M. J.; Aguilar, D. A.; Tsow, F.; Iglesias, R. A.; Zhang, Q.; Lu, J.; Li, J.; Tao, N. *J. Am. Chem. Soc.* **2009**, *131*, 1390–1391.
(14) Andrew, T. L.; Swager, T. M. *J. Am. Chem. Soc.* **2007**, *129*, 7254–7255.
(15) Narayanan, A.; Varnavski, O. P.; Swager, T. M.; Goodson III, T. *J. Phys. Chem. C* **2008**, *112*, 881–884.
(16) Freeman, R.; Willner, I. *Nano Lett.* **2009**, *9*, 322–326.
(17) Cerruti, M.; Jaworski, J.; Raorane, D.; Zueger, C.; Varadarajan, J.; Carraro, C.; Lee, S. K.; Maboudian, R.; Majumdar, A. *Anal. Chem.* **2009**, *81*, 4192–4199.
(18) Gao, D.; Wang, Z.; Liu, B.; Ni, L.; Wu, M.; Zhang, Z. *Anal. Chem.* **2008**, *80*, 8545–8553.
(19) Wang, S.; Singh, A. K.; Senapati, D.; Neely, A.; Yu, H.; Ray, P. C. *Chem. A- Eur. J.* **2010**, *16*, 5600–5606.
(20) Stewart, M. E.; Anderton, C. R.; Thompson, L. B.; Maria, J.; Gray, S. K.; Rogers, J. A.; Nuzzo, R. G. *Chem. Rev.* **2008**, *108*, 494–521.
(21) Ray, P. C. *Chem. Rev.* **2010**, *110*, 5332–5365.
(22) Griffin, J.; Singh, A. K.; Senapati, D.; Rhodes, P.; Mitchell, K.; Robinson, B.; Yu, E.; Ray, P. C. *Chem.—Eur. J.* **2009**, *15*, 342–351.
(23) Darbha, G. K.; Singh, A. K.; Rai, U. S.; Yu, E.; Yu, H.; Ray, P. C. *J. Am. Chem. Soc.* **2008**, *130*, 8038.
(24) Ray, P. C. *Angew. Chem., Int. Ed* **2006**, *45*, 1151–1154.
(25) Laurence, T. A.; Braun, G.; Talley, C.; Schwartzberg, A.; Moskovits, M.; Reich, N.; Huser, T. *J. Am. Chem. Soc.* **2009**, *131*, 162–169.
(26) Graham, D.; Thimpson, D. G.; Smith, W. E.; Faulds, K. *Nat. Nanotechnol.* **2008**, *3*, 548–551.
(27) Griffin, J.; Singh, A. K.; Senapati, D.; Lee, E.; Gaylor, K.; Jones-Boone, J.; Ray, P. C. *Small* **2009**, *5*, 839–845.
(28) Donath, E. *Nat. Nanotechnol.* **2009**, *4*, 215–216.
(29) Singh, A. K.; Senapati, D.; Wang, S.; Griffin, J.; Neely, A.; Candice, P.; Naylor, K. M.; Varisli, B.; Kalluri, J. R.; Ray, P. C. *ACS Nano* **2009**, *3*, 1906–1912.
(30) Darbha, G. K.; Singh, A. K.; Rai, U. S.; Yu, E.; Yu, H.; Ray, P. C. *J. Am. Chem. Soc.* **2008**, *130*, 8038.
(31) Qian, X.; Zhou, X.; Nie, S. *J. Am. Chem. Soc.* **2008**, *130*, 14934–14935.
(32) Kalluri, J. R.; Arbneshi, T.; Khan, S. F.; Neely, A.; Candice, P.; Varisli, B.; Washington, M.; McAfee, S.; Robinson, B.; Banerjee, S.; Singh, A. K.; Senapati, D.; Ray, P. C. *Angew, Chem, Int. Ed* **2009**, *48*, 9668–9671.
(33) Du, B. A.; Li, Z. P.; Liu, C. H. *Angew. Chem., Int. Ed* **2008**, *47*, 8022–8025.
(34) Ipe, B. I.; Shukla, A.; Liu, H.; Zou, B.; Rehage, H.; Niemeyer, C. M. *Chem. Phys. Chem* **2006**, *7*, 1112.
(35) Jans, H.; Liu, X.; Austin, L.; Maes, G.; Huo, Q. *Anal. Chem.* **2009**, *81*, 9425–9432.
(36) Camden, J. P.; Dieringer, J. A.; Wang, Y.; Masaiello, D. J.; Marks, L. D.; Schatz, G. C.; Van Duyne, R. P. *J. Am. Chem. Soc.* **2008**, *130*, 12616–12617.
(37) Mallouk, T. E.; Yang, P. *J. Am. Chem. Soc.* **2009**, *131*, 7937–7939.
(38) Qian, X.; Li, J.; Shuming, N. *J. Am. Chem. Soc.* **2009**, *131*, 7540–7541.
(39) Laurence, T. A.; Braun, G.; Talley, C.; Schwartzberg, A.; Moskovits, M.; Reich, N.; Huser, T. *J. Am. Chem. Soc.* **2009**, *131*, 162–169.
(40) Lal, S.; Clare, S. E.; Halas, N. J. *Acc. Chem. Res.* **2008**, *41*, 1842–1851.
(41) Jain, P. K.; Huang, X.; El-Sayed, I. H.; El-Sayed, M. A. *Acc. Chem. Res.* **2008**, *41*, 1578–1586.
(42) Stoeva, S. I.; Lee, J.-S.; Smith, J. E.; Rosen, S. T.; Mirkin, C. A. *J. Am. Chem. Soc.* **2006**, *128*, 8378–8379.
(43) Huang, X.; El-Sayed, I. H.; Qian, W.; El-Sayed, M. A. *J. Am. Chem. Soc.* **2006**, *128*, 2115–2120.
(44) Maeda, T.; Nakamura, R.; Kadckam, K.; Ohawa, H. I. *Environ. Toxicol. Chem.* **2007**, *25*, 237–241.

AM1005139